JHEP04(2014)011

ttH anomalous coupling in double Higgs production

Kenji Nishiwaki, Saurabh Niyogi and Ambresh Shivaji

Regional Centre for Accelerator-based Particle Physics, Harish-Chandra Research Institute, Chhatnag Road, Junsi, Allahabad-211019, India

E-mail: nishiwaki@hri.res.in, sourabh@hri.res.in, ambreshkshivaji@hri.res.in

ABSTRACT: We study the effects of top-Higgs anomalous coupling in the production of a pair of Higgs boson via gluon fusion at the Large Hadron Collider (LHC). The introduction of anomalous ttH coupling can alter the hadronic double Higgs boson cross section and can lead to characteristic changes in certain kinematic distributions. We perform a global analysis based on available LHC data on the Higgs to constrain the parameters of ttH anomalous coupling. Possible overlap of the predictions due to anomalous ttH coupling with those due to anomalous trilinear Higgs coupling is also studied. We briefly discuss the effect of the anomalous ttH coupling on the HZ production via gluon fusion which is one of the main backgrounds in the $HH \to \gamma\gamma b\bar{b}$ channel.

KEYWORDS: QCD Phenomenology, Hadronic Colliders

ARXIV EPRINT: 1309.6907

Contents

1 Introduction

The discovery of Higgs boson by the Large Hadron Collider (LHC) [1, 2] at CERN once again writes the great success story of the standard model (SM). Though it is not yet conclusively declared that this is the 'very' Higgs boson postulated in the standard model, but more data consolidate the same. However, there are still room left for new physics to show up at the weak scale within the reach of the LHC. There are many ways to search for new physics at the LHC. The most popular one is to look for new resonances directly produced in proton-proton collision. But no such new particles have been found till date. Hence, lower limits at 95% confidence level (CL) has been placed constraining various models of new physics. The other way is to look for deviation in couplings where new physics effects may enter. It will, in turn, show up in appropriate production or decay processes at the LHC. We shall take this latter approach in a model independent way to probe the nature of new physics. In fact, after the discovery of the Higgs boson, it still remains to verify its couplings with other standard model particles and also with itself. Recent studies involving anomalous couplings of the Higgs boson at the LHC have been reported in [3–19]. Prospects of the measurement potential of various Higgs couplings at future linear collider are also discussed in ref. [20].

In the standard model, the couplings of the Higgs boson with the fermions and gauge bosons are proportional to their masses. Its large $\sim O(1)$ coupling with top quark is the reason for expecting that any deviation, if present, might show up via top-Higgs coupling. Hence, probing this coupling always remains a priority. The top-Higgs Yukawa coupling can be indirectly probed by the measurements of inclusive Higgs boson production which is dominated by gluon fusion process and also in the decay of the Higgs to diphoton and digluon channels mediated by the top quark loop. However, the only direct way to constrain this coupling is to measure ttH production at the LHC. ATLAS and CMS has

already published data in this direction, but not much deviation from the standard model has been observed. Given the theoretical and experimental uncertainties, it is difficult to derive any meaningful limit from the collected data [21, 22].

Due to the presence of new physics the top-Higgs coupling can differ from its standard model value [23–26]. These deviations can come from higher dimensional operators present below a certain scale [22, 27–29]. Moreover, many of the new physics models also predict deviation in ttH coupling from the standard one. The standard model Higgs boson is predicted to be CP-even. However, LHC data do not rule out the Higgs to be a mixed CP state. Taking this freedom, we consider top-Higgs coupling to be CP-violating one for this work. We stress that we do not focus on some specific model or some set of effective operators. Instead, we consider a general parameterization of anomalous top-Higgs coupling which definitely includes all the above effects.

Double Higgs production at the LHC provides a good opportunity to probe various couplings of the Higgs boson. Since gluon fusion is still the dominant channel for Higgs pair production, just like single Higgs production, this process has strong dependence on ttH coupling. At the same time, it can give access to the Higgs trilinear coupling as well.

This paper is organized as follows. In the following section 2, we discuss the Higgs pair production in the standard model itself. In section 3, the general parameterization of top-Higgs interaction is motivated. This will be followed by the effects of anomalous coupling on the production cross section and on different kinematic variables of the Higgs pair production at the LHC. Next, section 5 will consist of the constraints from the LHC experiments and resultant global analysis. Finally in section 6, we summarize our observations and give careful consideration to the prospects of the Higgs pair production based on the results of the global analysis.

## 2 Higgs pair production in the standard model

The Higgs boson pair production within the standard model was first studied in [30, 31]. Very much like the production of single Higgs boson, the gluon fusion channel is the dominant mode to produce a pair of Higgs boson at hadron colliders. At the leading order the process proceeds via quark loop diagrams, shown in figure 1.[1] The major contribution to the hadronic cross section comes from the top quark loop diagram. The bottom quark loop contribution is well below 1% (0.2% at 14 TeV) of the total cross section. One of the important features of this process is the destructive interference that takes places between the box and the triangle contributions.[2] The two contributions are separately gauge invariant. As we can see in figure 2, the destructive interference effect is quite strong. For example, at 14 TeV, the separate contributions of the triangle and box amplitudes towards the total hadronic cross section is about 6.98 fb and 54.22 fb respectively. The net cross section, on the other hand, is only 26.50 fb, i.e., there is a reduction of more than 50% in the cross section due to the interference term. Note that the minimum threshold to produce the Higgs

---

[1]These diagrams are drawn using the Jaxodraw package [32].

[2]We use, $\sigma = \sigma_{tr} + \sigma_{bx} - \sigma_{int}$, where σ_{int} is due to the interference between the triangle and box amplitudes.
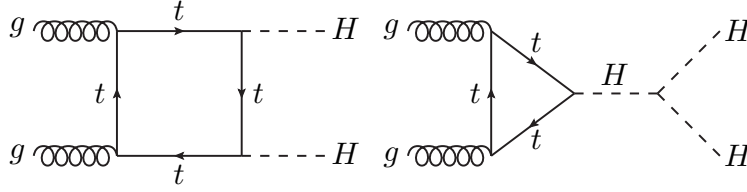
Figure 1. Prototype diagrams for the leading order production of double Higgs via gluon fusion. Other diagrams are generated by permuting the external legs appropriately.
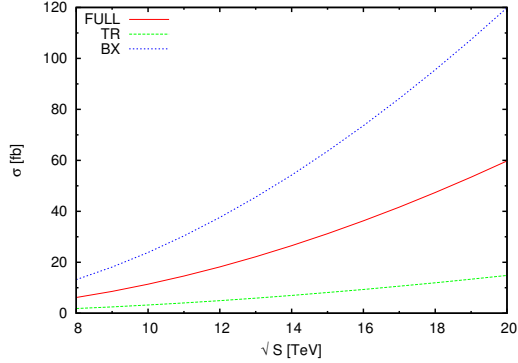
Figure 2. Triangle (TR) and box (BX) amplitudes contributions to the hadronic cross sections at various collider center-of-mass energies in the standard model.
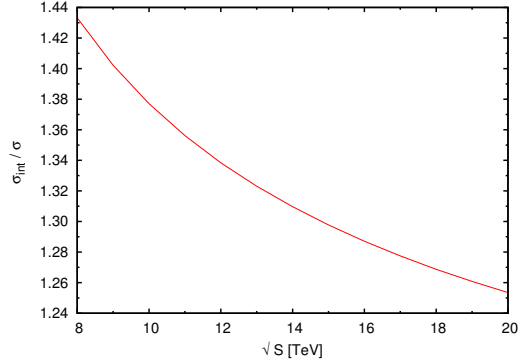
Figure 3. Fractional contribution of the cross section due to the interference term at various collider center-of-mass energies in the standard model.

boson pair is greater than the Higgs mass, therefore, the intermediate Higgs boson in the triangle diagram is always off-shell. We expect that due to the propagator suppression in the triangle amplitude, the interference effect falls at higher energies, see figure 3.

Higgs pair production has also been a subject of discussion in the context of various new physics models [33–36] including the minimal supersymmetric standard model (MSSM) [37] and the Little Higgs [38, 39]. Total Higgs pair production cross section including higher order corrections has been discussed in [40–44]. It is known that in the large fermion mass limit the amplitude does not vanish. This non-decoupling behaviour makes the process sensitive to the existence of heavier quarks in new physics models [45]. The process is also important from the point of view of measuring the trilinear self-coupling of the Higgs boson [46] which is present in the triangle diagram of figure 1. The precise measurement of the trilinear self-coupling of the Higgs boson is required to confirm the form of the scalar potential responsible for the electroweak symmetry breaking. However, the collider center-of-mass energy and the luminosity required to observe this channel at the LHC has not been reached yet.

3 The top-Higgs anomalous coupling

It is well known that the absolute sign of the standard model Yukawa coupling is arbitrary. Nevertheless, its relative sign with respect to the mass term is completely determined. Any

change in this relative sign will be a clear indication of new physics effects. At the same time, this change in the relative sign can have serious implications for those processes which involve both ttH and any of the three couplings HWW, HZZ and HHH. Plausibility of such scenarios has been considered in associated production of a single top and a Higgs boson at the LHC [47–50]. Since, the Higgs pair production process involves both the top-Yukawa coupling and the trilinear Higgs coupling, the relative sign change between the two couplings will lead to constructive interference between the box and the triangle contributions. As a result the Higgs pair production rates at the LHC will be higher as compared to those predicted in the standard model. In addition to that, the presence of new physics can also modify the nature of various standard model couplings. The top-quark being exceptionally heavy as compared to the other fermions may hold the signatures of new physics. In the standard model, the top-Yukawa coupling is purely scalar type. Many new physics models, such as the composite Higgs models [51] and models with the extended Higgs sector [52] suggest that the Yukawa couplings can be an admixture of both the scalar and pseudoscalar type of couplings. In other words, the physical Higgs boson may not have a definite CP property [53].

A phenomenological Lagrangian describing the nonstandard top quark Yukawa coupling can be parameterized as,

$$\mathcal{L}_{\text{ttH}} = -\frac{g_w m_t}{2M_w} \ \bar{t}(a + ib\gamma^5)t \ H, \tag{3.1}$$

where g_w is the SU(2) gauge coupling constant. Both the dimensionless parameters a and b are real and they assume values 1 and 0 respectively in the standard model at the leading order. The γ^5 or the pseudoscalar part of the coupling has to be imaginary due to the hermiticity of the Lagrangian. Since, CP is not an exact symmetry of the standard model, the CP-odd term, in principle, can be generated at higher loops. However, such contributions are expected to be very small within the standard model. The above form of the top-Higgs coupling can also be motivated in the effective Lagrangian approach to new physics studies. In this approach the new physics effects can be parameterized by a set of gauge invariant higher dimensional operators involving the standard model fields only. We can write down an effective Lagrangian using these operators as,

$$\mathcal{L}_{\text{eff}} = \sum_i \frac{C_i}{\Lambda^{d_i-4}} \mathcal{O}^i, \tag{3.2}$$

where $d_i > 4$ is the mass dimension of the operator $\mathcal{O}^i$, the free parameter C_i fixes the strength of the corresponding operator and Λ is the cutoff scale above which this effective description of new physics is not valid. These higher dimensional operators can modify both the strength and the nature of various standard model couplings. For example, the *lowest* higher dimensional operators which contribute to the top-Higgs Yukawa coupling are dimension-six operators [22, 28, 29] and these are given by

$$(\Phi^\dagger\Phi)(\bar{Q}_L t_R \tilde{\Phi}) \ ; \ (\Phi^\dagger\sigma^I D_\mu\Phi)(\bar{Q}_L\gamma^\mu\sigma^I Q_L) \ ; \ (\Phi^\dagger D_\mu\Phi)(\bar{Q}_L\gamma^\mu Q_L) \ ; \ (\Phi^\dagger D_\mu\Phi)(\bar{t}_R\gamma^\mu t_R).$$
$$\tag{3.3}$$

In the above, Φ ($\tilde{\Phi} = i\sigma_2\Phi^*$) is the standard model Higgs doublet field, $\bar{Q}_L = (\bar{t}_L, \bar{b}_L)$ is the third generation quark doublet, t_R is the top quark singlet and $\sigma^I(I = 1, 2, 3)$ are the 2×2 Pauli matrices. As a result of the electroweak symmetry breakdown, the field Φ obtains a vacuum expectation value and the above operators effectively generate deviations in the parameters of eq. (3.1) away from their standard model values. We can assume similar parameterization for other Yukawa couplings also. However, for our process under consideration, it is the top-Yukawa coupling which is the most relevant.

At present, there are no significant *direct* bounds on the anomalous top-Higgs coupling parameters from the collider experiments. In ref. [54] unitarity constraints on these parameters are derived assuming the new physics scale at $1\,\mathrm{TeV}$ which allow $O(1)$ values for the parameters. Note that the parametric form of the anomalous ttH coupling in eq. (3.1) violates the CP symmetry explicitly for non-zero b. The CP-odd part of the coupling contributes to both the electroweak baryogenesis and the electric dipole moments (EDMs) of fermions [55–57]. We can use the measurements of the EDMs of the electron and the neutron to place indirect bounds on the parameter b. In ref. [57], the EDM bounds on b are found to be of $O(0.01)$. This bound can be circumvented if the electron, up and down quark Yukawa couplings are also anomalous. The phenomenology of top-Higgs anomalous coupling under consideration has been studied at both the linear [55, 58] and hadron colliders [59, 60]. Now we consider the effect of top-Higgs anomalous coupling on the Higgs pair production process, keeping all the other standard model couplings intact. However, in section 6, we will briefly discuss the effect of anomalous trilinear Higgs coupling in the same process.

## 4 Higgs pair production in presence of anomalous ttH coupling

The full amplitude of our process in presence of the anomalous ttH coupling can be expressed in the following form,

$$\mathcal{M} = a^2\mathcal{M}^{\mathrm{SM}}_{bx} + b^2\mathcal{M}^{(1)}_{bx} + ab\mathcal{M}^{(2)}_{bx} + a\mathcal{M}^{\mathrm{SM}}_{tr} + b\mathcal{M}^{(3)}_{tr}. \tag{4.1}$$

We consider this structure of the amplitude after computing the quark loop traces of the diagrams. Here, $\mathcal{M}^{\mathrm{SM}}_{bx/tr}$ are the standard model values of the box (bx) and triangle (tr) amplitudes and $\mathcal{M}^{(\mathrm{i})}_{bx/tr}$ are the additional box and triangle contributions due to the pseudoscalar coupling of the Higgs boson with the top quark. The terms linear in b in the above amplitude are proportional to possible ϵ-tensor structures such as $\epsilon(p_i, p_j, e_1, e_2)$ and $\epsilon(p_1, p_2, p_3, e_i)$, where e_is are the polarization vectors of the gluons.[3] The amplitude-squared will also have terms odd in b. However, once the gluon polarizations are summed over, such terms in the amplitude-squared vanish due to the 4-momentum conservation. Thus the unpolarized cross section of the two Higgs production process is expected to depend only on the absolute value of the parameter b. On the other hand, a change in sign in the parameter a leads to significant changes in results discussed below.

---

[3]$\epsilon(p_1, p_2, e_1, e_2) = \epsilon^{\mu\nu\alpha\beta}p_{1\mu}p_{2\nu}e_{1\alpha}e_{2\beta}$.
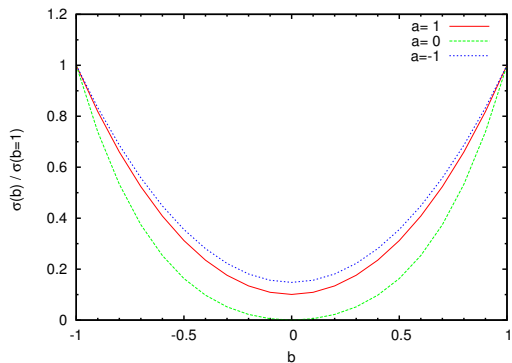
Figure 4. Cross sections as function of parameter b for $a = 1, 0, -1$. We have scaled the cross sections in all the three cases by their maximum values at $b = 1$. The symmetry of these plots about $b = 0$ is explained in the text.
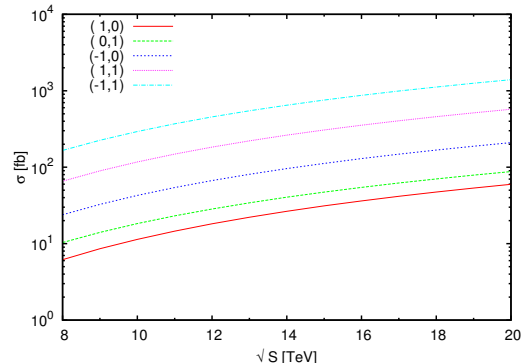

Figure 5. Dependence of cross section on the collider center-of-mass energy for various combinations of anomalous ttH coupling parameters (a, b).

| $\sqrt{S}$ (TeV)	$\sigma_{(1,0)}$ (fb)	$\sigma_{(0,\pm 1)}$ (fb)	$\sigma_{(-1,0)}$ (fb)	$\sigma_{(1,\pm 1)}$ (fb)	$\sigma_{(-1,\pm 1)}$ (fb)
8	6.18	10.34	23.89	65.58	165.89
14	26.50	40.53	95.91	262.82	648.05
33	167.51	234.94	567.27	1549.86	3719.29

Table 1. $gg \to HH$ leading order hadronic cross sections for various combinations of parameters (a, b).

We have adopted a semi-numerical approach to calculate the one-loop amplitude. The quark loop traces for the box and triangle diagrams involving anomalous ttH coupling are calculated using FORM in four dimensions [61]. The one-loop tensor integrals which appear in the amplitude are reduced into one-loop scalars following the Oldenborgh and Vermaseren (OV) method [62]. The scalar integrals are calculated using the OneLOop package [63]. We calculate helicity amplitudes numerically before squaring them to obtain the total and differential cross sections. The numerical results presented in this section use CTEQ6L1 parton distribution functions [64]. We have taken $\mu = M_H(= 125\,\text{GeV})$ as the common scale of renormalization and factorization. We have not applied any kinematic cuts on the final state particles.

In figure 4, we can clearly see enhancement in the hadronic cross section due to the anomalous coupling parameters a and b. In pure pseudoscalar case ($a = 0, b \neq 0$), only the box diagrams contribute to the unpolarized cross section. For $a = -1$, the two diagrams in figure 1 interfere constructively leading to more than three fold increment in the cross section. The cross section is indeed insensitive to any sign change in b. We have further shown the cross sections for some benchmark values of (a, b) as function of collider center-of-mass energy in figure 5. For convenience, some of the numbers of interest are also
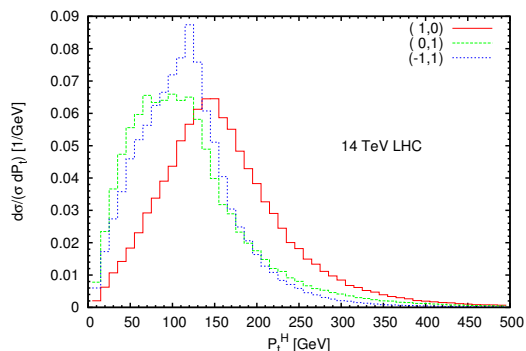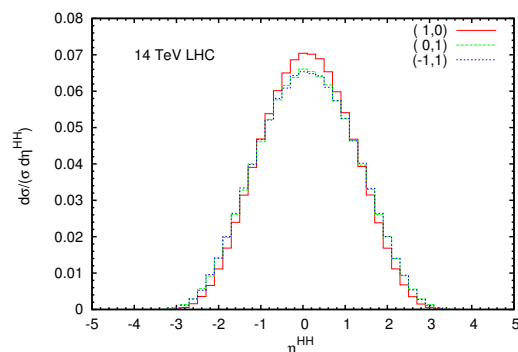
Figure 6. Normalized P_t-distributions of the Higgs for various combinations of anomalous ttH coupling parameters (a, b).
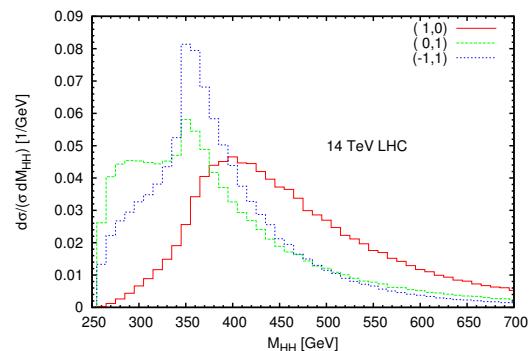
Figure 7. Normalized two Higgs invariant mass distributions for various combinations of anomalous ttH coupling parameters (a, b).
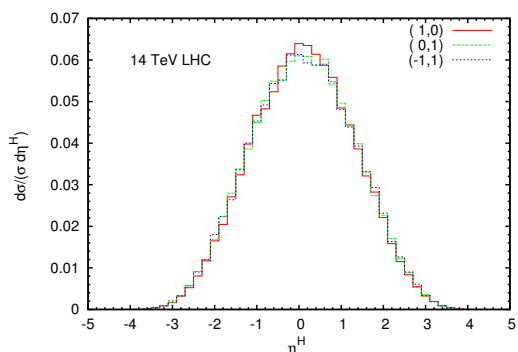
Figure 8. Normalized rapidity distributions of the Higgs for various combinations of anomalous ttH coupling parameters (a, b).
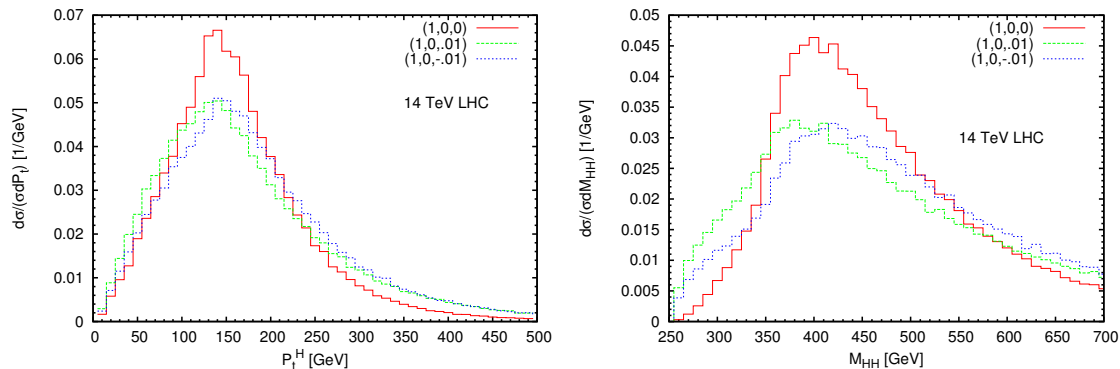

Figure 9. Normalized rapidity distributions of the two Higgs system for various combinations of anomalous ttH coupling parameters (a, b).

given in the table 1. Although, these benchmark values may not be realistic in the light of present LHC data on the Higgs-like particle, we consider them here for book keeping purpose. Apart from enhancing the production cross section, these anomalous couplings also lead to characteristic changes in certain kinematic distributions. The distributions are presented for 14 TeV LHC.

In figure 6, we have compared the normalized transverse momentum distributions of Higgs plotted for certain benchmark values of parameters (a, b). We find that in presence of anomalous couplings, the contribution from phase space region with P_t^H below 150 GeV increases significantly. Similar conclusions are drawn from the invariant mass (M_{HH}) distributions of the two Higgs bosons displayed in figure 7. The distributions start at $M_{HH} = 2M_H$ which is the production threshold for the two Higgs bosons in the final state. In the standard model case, there is an exact cancellation between the box and the triangle contributions in the large m_t limit [30]. This is clearly reflected in the low invariant mass region of the standard model distribution where large m_t limit is a good approximation. Any deviation in the parameters (a, b) beyond standard model values dilutes this fine cancellation. The enhancement near $M_{HH} = 2m_t$ $(m_t = 172\,\text{GeV})$ threshold is also visible

– 7 –

Figure 10. Effect of $ttHH$ coupling on normalized P_t and invariant mass distributions in double Higgs production. At $14\,\mathrm{TeV}$, for $c = -0.01$ and 0.01 the cross sections are $319.00\,\mathrm{fb}$ and $221.03\,\mathrm{fb}$ respectively.

in these distributions. The rapidity distributions do not deviate much from the standard model case, see figures 8 and 9. Similarly, the distribution corresponding to $\theta_{HH}^{\star}$ variable, discussed in section 4 of ref. [41], does not show any significant deviation.

We would like to mention that in the context of the double Higgs production, the top-Higgs anomalous coupling can have more general features in addition to what is considered in eq. (3.1). For example, in the effective Lagrangian approach, the operators shown in eq. (3.3) also generate $ttHH$ contact interaction and it is related to the parameters of the ttH coupling. Such contact interaction terms are also common in composite Higgs models [34]. This new interaction can lead to drastic increment in the cross section of the double Higgs production, especially when the value of Λ is quite low [27]. If we parametrize the $ttHH$ coupling factor by $(-m_t/v^2)c$ with a dimensionless parameter c, we find that for $c \gtrsim 0.001$ the effects are visible in both the cross section as well as in the transverse momentum and invariant mass distributions. As an illustration the normalized distributions for $c = \pm 0.01$ are given in figure 10 keeping a and b fixed at their standard model values. Moreover, the anomalous couplings of the top quark with gluons and those of the Higgs boson with the gluons can also modify the Higgs pair production cross section at the LHC [29]. In presence of large number of free parameters, we loose the predictability and it becomes difficult to disentangle the effect of a specific parameter. To avoid this ambiguity we have not included any other anomalous coupling in our study.

5   Constraints from LHC experiments

The LHC data on Higgs boson can be, in principle, used to constrain all those couplings which can affect the main production and/or decay channels of a single Higgs boson. However, we are interested in the couplings of the Higgs with fermions and gauge bosons which might be sensitive to new physics. In this regard, ttH, WWH and ZZH couplings are the most relevant ones. Just like the sources of anomalous term in case of ttH, similar higher dimensional operators could modify WWH/ZZH couplings as well. However, we note that such anomalous couplings of Higgs with gauge bosons are already constrained

by the electroweak precision data.[4] Also, $H \to WW^*$ and $H \to ZZ^*$ are the two crucial channels in which Higgs boson has been observed at the LHC. Therefore, these couplings get directly constrained by the observed data. Hence, we do not intend to introduce any modifications to these couplings. In this section, we discuss the constraints on the anomalous top Yukawa parameters from the latest results of Higgs searches at the LHC.

The LHC experiments have collected data in the production channels which include the gluon fusion, the vector boson fusion, the Higgs-strahlung (associated production with a W/Z-boson), and the associated production with a pair of top quarks. Under the existence of the top-Higgs anomalous coupling as shown in eq. (3.1), both the single Higgs production via gluon fusion and the Higgs production in association with $t\bar{t}$ are altered. In addition to that, the partial decay widths of the Higgs to diphoton ($\Gamma_{H \to \gamma\gamma}$) and digluon ($\Gamma_{H \to gg}$) are deviated from those of the standard model values ($\Gamma_{H \to \gamma\gamma}^{\rm SM}$, $\Gamma_{H \to gg}^{\rm SM}$). The top-Higgs anomalous coupling also modifies the $H \to Z\gamma$ decay width. But this channel is hard to reconstruct and the constraints are still loose [65, 66]. The branching ratio of this decay mode in standard model itself is small. Hence we do not expect sizable deviation of the total Higgs decay width coming from this channel. Therefore, we totally ignore the effects on $H \to Z\gamma$ due to the top-Higgs anomalous coupling in this paper.

In presence of anomalous top Yukawa coupling, the analytical expressions of the decay widths, $\Gamma_{H \to gg}$ and $\Gamma_{H \to \gamma\gamma}$, are given by

$$\Gamma_{H \to gg} = \frac{G_F \alpha_s^2 M_H^3}{36\sqrt{2}\pi^3} \left\{ \left| \frac{3}{4} a A_{1/2}(\tau_t) + \frac{3}{4} A_{1/2}(\tau_b) \right|^2 + \left| \frac{3}{4} \times 2b \frac{f(\tau_t)}{\tau_t} \right|^2 \right\}, \tag{5.1}$$

$$\Gamma_{H \to \gamma\gamma} = \frac{G_F \alpha^2 M_H^3}{128\sqrt{2}\pi^3} \left\{ \left| A_1(\tau_W) + a N_C Q_t^2 A_{1/2}(\tau_t) + N_C Q_b^2 A_{1/2}(\tau_b) \right|^2 \right.$$
$$\left. + \left| N_C Q_t^2 \times 2b \frac{f(\tau_t)}{\tau_t} \right|^2 \right\}, \tag{5.2}$$

with the functions of τ_i as in ref. [67], which is defined as $\tau_i \equiv M_H^2 / 4M_i^2$,

$$f(\tau_i) = \begin{cases} \arcsin^2(\sqrt{\tau_i}) & \tau_i \leq 1, \\ \\ -\frac{1}{4} \left[\log \frac{1 + \sqrt{1 - \tau_i^{-1}}}{1 - \sqrt{1 - \tau_i^{-1}}} - i\pi \right]^2 & \tau_i > 1, \end{cases} \tag{5.3}$$
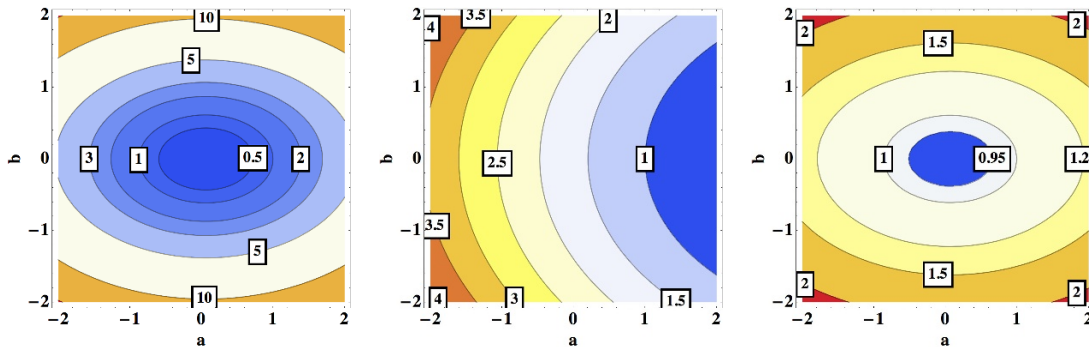
$$A_{1/2}(\tau_i) = \frac{2}{\tau_i^2} \left[\tau_i + (\tau_i - 1) f(\tau_i) \right], \tag{5.4}$$

$$A_1(\tau_i) = -\frac{1}{\tau_i^2} \left[2\tau_i^2 + 3\tau_i + 3(2\tau_i - 1) f(\tau_i) \right]. \tag{5.5}$$

Here G_F is the Fermi constant, α_s and α are the fine structure constants for QCD and QED, and N_C, $Q_t(Q_b)$ represent the QCD color factor and electric charge of the top(bottom)

---

[4]We note that there is no additional contribution to the Peskin-Takeuchi S, T, U parameters due to the anomalous ttH coupling at 1-loop level.

Figure 11. The deviations of $\Gamma_{H\to gg}/\Gamma_{H\to gg}^{\rm SM}$(left), $\Gamma_{H\to\gamma\gamma}/\Gamma_{H\to\gamma\gamma}^{\rm SM}$(center) and $\Gamma_H/\Gamma_H^{\rm SM}$(right) as functions of a and b, respectively.

quark, respectively. Note that we also include the contribution from the bottom quark since the corresponding loop function $A_{1/2}(\tau_b)$ is non-negligible.

As mentioned earlier, $\Gamma_{H\to gg}$ and $\Gamma_{H\to\gamma\gamma}$ and hence, total Higgs decay width Γ_H change from their standard model values due to the presence of modified ttH coupling. The following ratio is suitable for evaluating this effect:

$$\frac{\Gamma_H}{\Gamma_H^{\rm SM}} = {\rm Br}_{H\to{\rm others}}^{\rm SM} + \frac{\Gamma_{H\to gg}}{\Gamma_{H\to gg}^{\rm SM}}{\rm Br}_{H\to gg}^{\rm SM} + \frac{\Gamma_{H\to\gamma\gamma}}{\Gamma_{H\to\gamma\gamma}^{\rm SM}}{\rm Br}_{H\to\gamma\gamma}^{\rm SM}, \tag{5.6}$$

where ${\rm Br}_{H\to{\rm others}}^{\rm SM} = 0.913$, ${\rm Br}_{H\to gg}^{\rm SM} = 0.085$ and ${\rm Br}_{H\to\gamma\gamma}^{\rm SM} = 0.002$ are the branching ratios at around $M_H = 125\,{\rm GeV}$ in the standard model [68]. We assume that the K-factors are the same as those in the standard model and are dropped in eq. (5.6). Figure 11 shows the deviations of $\Gamma_{H\to gg}/\Gamma_{H\to gg}^{\rm SM}$, $\Gamma_{H\to\gamma\gamma}/\Gamma_{H\to\gamma\gamma}^{\rm SM}$ and $\Gamma_H/\Gamma_H^{\rm SM}$ as functions of the top-Higgs anomalous parameters a and b. The three ratios are more sensitive to the parameter b compared to a because of the largeness of the loop function, $A_{1/2}(\tau_t) \simeq 1.4$ and $2f(\tau_t)/\tau_t \simeq 2.1$. In negative region of a, due to the constructive interference of W and the quark loop contributions, the deviation in $\Gamma_{H\to\gamma\gamma}/\Gamma_{H\to\gamma\gamma}^{\rm SM}$ turns out to be significant. Because the value of ${\rm Br}_{H\to gg}^{\rm SM} = 0.085$ is not so small, the ratio of the total width $\Gamma_H/\Gamma_H^{\rm SM}$ receives a sizable modification in the region where $\Gamma_{H\to gg}/\Gamma_{H\to gg}^{\rm SM}$ is large.

Now, we address the deviations in cross sections of the single Higgs production processes due to the top-Higgs anomalous coupling. The leading order cross section in gluon fusion channel can be evaluated from:

$$\hat{\sigma}_{gg\to H} = \frac{\pi^2}{8M_H}\Gamma_{H\to gg}\delta(\hat{s} - M_H^2), \tag{5.7}$$

where the hat symbol indicates that it is a parton level value. The form in eq. (5.7) suggests that, at the hadron level, the parton-distribution part should be factorized and we can conclude the following relation:

$$\frac{\sigma_{gg\to H}}{\sigma_{gg\to H}^{\rm SM}} = \frac{\Gamma_{H\to gg}}{\Gamma_{H\to gg}^{\rm SM}}. \tag{5.8}$$

Therefore, the left most plot in figure 11 also represents deviations in $gg \to H$ cross section in presence of anomalous coupling parameters a and b. For calculating the deviation

$\sigma_{pp \to t\bar{t}H}/\sigma_{pp \to t\bar{t}H}^{\mathrm{SM}}$, we implement the anomalous coupling with the help of FeynRules [69] and generate a Universal FeynRules Output (UFO) model file [70] for Madgraph 5 [71]. The left contour plot of figure 12 shows the ratio $\sigma_{pp \to t\bar{t}H}/\sigma_{pp \to t\bar{t}H}^{\mathrm{SM}}$ as a function of a and b at $\sqrt{s} = 8\,\mathrm{TeV}$, which is symmetric under $a \to -a$ or $b \to -b$ and the effect of b is subleading in contradiction to $gg \to H$, $H \to gg$ and $H \to \gamma\gamma$. We use the CTEQ6L1 parton distribution function for calculating the cross section. Both the renormalization and factorization scales have been set at $(2m_t + M_H)$.

The ATLAS and the CMS experiments have published the inclusive results of $H \to \gamma\gamma$, $H \to ZZ^* \to 4\ell$ and $H \to WW^* \to 2\ell 2\nu$ for each category tagging their decays [72–77], where all the production channels are considered. Also, $H \to b\bar{b}$ after the production through the vector boson fusion [78] and the Higgs-strahlung [79, 80] have been reported. We can put a bound on the (a, b)-plane after executing a global analysis based on the above data.[5] On the other hand, the signal strength of $pp \to t\bar{t}H$ (subsequently, $H \to \gamma\gamma$ or $H \to b\bar{b}$) is now constrained at the LHC. The ATLAS have claimed that at the 95% CL the observed upper limits from $H \to \gamma\gamma$ and $H \to b\bar{b}$ are 5.3 [81] and 13.1 [82] respectively, while the CMS counterparts are 5.4 ($H \to \gamma\gamma$) [83] and 5.8 ($H \to b\bar{b}$) [84]. Since, the top-Higgs anomalous coupling can modify these sequences of production and decay, additional restrictions on a and b can be imposed. Due to the large uncertainties, we do not use these data in our global analysis and separately examine a bound from this channel without considering errors seriously. The right plot in figure 12 represents the regions where the results are consistent with the CMS observations; $\mu_{pp \to t\bar{t}H, H \to \gamma\gamma} \leq 5.4$ (cyan) or $\mu_{pp \to t\bar{t}H, H \to b\bar{b}} \leq 5.8$ (magenta). The tendency of the two constraints can be understood from the properties of the three fractions $\Gamma_{H \to gg}/\Gamma_{H \to gg}^{\mathrm{SM}}$, $\Gamma_{H \to \gamma\gamma}/\Gamma_{H \to \gamma\gamma}^{\mathrm{SM}}$ and $\Gamma_H/\Gamma_H^{\mathrm{SM}}$ which we discussed before. The purple area is the superposition of the two allowed regions.

In order to take into account the difference in the production processes in our global analysis, we employ the following weight used in refs. [85, 86]:

$$\epsilon_f^{I,X} = \frac{a_f^{I,X} \sigma_X^{\mathrm{SM}}}{\sum_Y a_f^{I,Y} \sigma_Y^{\mathrm{SM}}}, \tag{5.9}$$

where X and I are indices to distinguish the production channels and event categories in the decay $H \to f$, σ_X^{SM} is the single Higgs production cross section of the channel X in the standard model, and $a_f^{I,Y}$ means acceptances. After ignoring the deviations in acceptances originating from effects of new physics, we can identify the weight factor $\epsilon_f^{I,X}$ as the fractions of expected signal events from the five production processes, whose details are provided in refs. [72–77, 87] and summarized in section 3 of ref. [85]. Note that the simple relation $\sum_X \epsilon_f^{I,X} = 1$ holds. After the set $\{\epsilon_f^{I,X}\}$ is ready in the decay $H \to f$, the signal strength can be written down as follows:

$$\mu_{H \to f}^I = \sum_X \epsilon_f^{I,X} \frac{\sigma_X}{\sigma_X^{\mathrm{SM}}} \frac{\mathrm{Br}_{H \to f}}{\mathrm{Br}_{H \to f}^{\mathrm{SM}}} = \sum_X \epsilon_f^{I,X} \frac{\sigma_X}{\sigma_X^{\mathrm{SM}}} \frac{\Gamma_{H \to f}}{\Gamma_{H \to f}^{\mathrm{SM}}} \frac{\Gamma_H^{\mathrm{SM}}}{\Gamma_H}, \tag{5.10}$$

---

[5]Lots of works have been done before and after the Higgs discovery. See e.g., refs. in [3–19] for recent status.
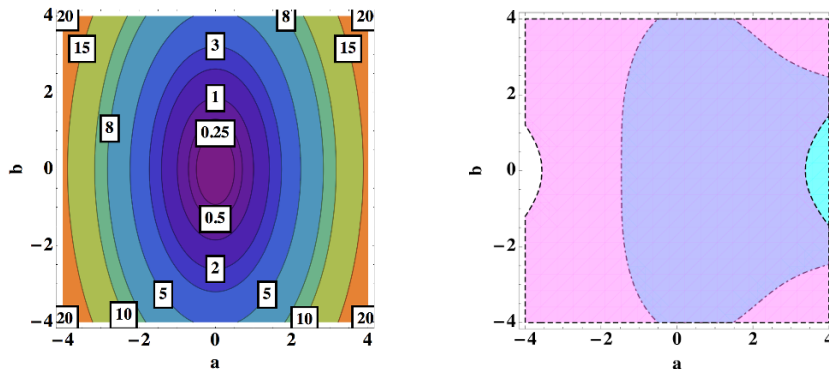
Figure 12. *Left:* $\sigma_{pp \to t\bar{t}H}/\sigma^{\rm SM}_{pp \to t\bar{t}H}$ as a function of a and b at $\sqrt{s} = 8\,{\rm TeV}$. *Right:* parameter regions being consistent with the CMS observations; $\mu_{pp \to t\bar{t}H, H \to \gamma\gamma} \leq 5.4$ (cyan) [83] or $\mu_{pp \to t\bar{t}H, H \to b\bar{b}} \leq 5.8$ (magenta) [84]. The purple area is the superposition of the two allowed regions.

| Type	Signal strength	Reference
ATLAS, VH(bb), 0 lepton	$0.5^{+0.9}_{-0.9}$	
ATLAS, VH(bb), 1 lepton	$0.1^{+1.0}_{-1.0}$	[79]
ATLAS, VH(bb), 2 lepton	$-0.4^{+1.5}_{-1.4}$	
CMS, $Z(\nu\nu)H(bb)$	1.04 ± 0.77	
CMS, $Z(\ell^+\ell^-)H(bb)$	0.82 ± 0.97	[80]
CMS, $Z(\ell\nu)H(bb)$	1.11 ± 0.87	
CMS, H(bb) from VBF	0.7 ± 1.4	[78]

Table 2. Details of 7 observables of $H \to b\bar{b}$ after the production through the vector boson fusion and the Higgs-strahlung.

where σ_X represents the Higgs production cross section of the process X with the top-Higgs anomalous coupling, and ${\rm Br}^{\rm (SM)}_{H \to f} = \Gamma^{\rm (SM)}_{H \to f}/\Gamma^{\rm (SM)}_H$ is the branching ratio of the Higgs decay channel $H \to f$ (in the standard model). The possible deviations via loop corrections of the ratios, $\Gamma_{H \to f}/\Gamma^{\rm SM}_{H \to f}$ and $\Gamma^{\rm SM}_H/\Gamma_H$ are already evaluated in eqs. (5.1), (5.2) and (5.6). We mention that all the other ratios have no deviation from the standard model. As mentioned earlier, the ratio $\sigma_X/\sigma^{\rm SM}_X$ deviates from one only in the gluon fusion production channel and in $pp \to t\bar{t}H$ production channel.

Next, we perform a χ^2 analysis with the ATLAS and the CMS results with the χ^2 function defined as

$$\chi^2 = \sum_f \sum_I \left(\frac{\mu^I_{H \to f} - \hat{\mu}^I_f}{\hat{\sigma}^I_f} \right)^2 . \tag{5.11}$$

We assume every experimental result follows Gaussian distribution ($\hat{\mu}^I_f \pm \hat{\sigma}^I_f$) and ignore the correlations among the event categories, which are not yet published. When an error is asymmetric, we adopt its simple average as the value of the corresponding $\hat{\sigma}^I_f$. We use 42 observables of $H \to \gamma\gamma$ [72, 75], $H \to ZZ^* \to 4\ell$ [73, 76], and $H \to WW^* \to 2\ell 2\nu$ [74, 77],
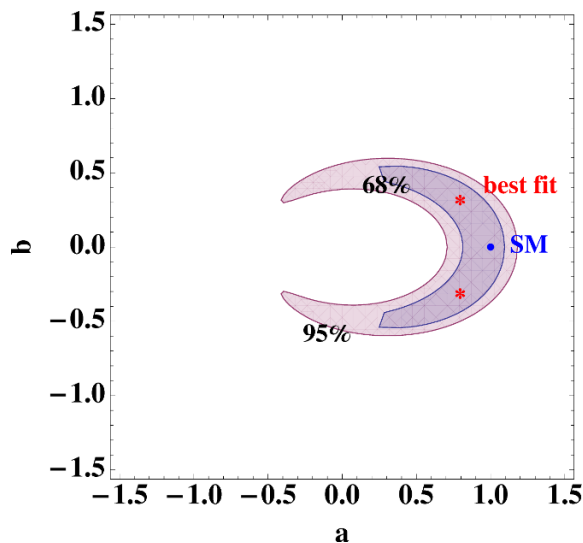
Figure 13. 68% and 95% CL allowed regions of the global analysis. The red asterisks and the blue point represent the best-fit point and the standard model point, respectively.

whose details are summarized in section 3 of ref. [85], and 7 ones of $H \to b\bar{b}$ after the production through the vector boson fusion [78] and the Higgs-strahlung [79, 80], where we can find the values in table 2. We note that the number of the inputs is 49 in total. The 68% and 95% CL allowed regions are shown in figure 13, where the best-fit point (global minimum of χ^2) is found at $(a, b) = (0.796, \pm 0.315)$ with $\chi^2_{\min} = 36.0$. The large area near the point $(0, 0)$ in the (a, b)-plane is disfavored because the dominant single Higgs production via gluon fusion is suppressed much and this is in contradiction to the (inclusive) experimental results. The anomalous coupling b is more restricted than a since deviation of b plays the primary role in the single Higgs production and its decay. We mention that, after combining the result of our global analysis with the constraint from the $pp \to t\bar{t}H$, which is shown in figure 12, the favored region does not change.

We should mention that this estimation is rather crude because of lack of error consideration. We hope that we can be more confident on our results after accumulation of further data in $pp \to t\bar{t}H$ process in the near future. We should also emphasize that we only consider anomalous couplings in the top Yukawa sector in the global analysis. After introducing deviations in other couplings, the result might get modified.

6 Summary and discussions

In this paper, we consider anomalous ttH coupling and explore its effects on the Higgs pair production at the LHC. The term 'anomalous' is an indication of possible new physics beyond the standard model. This anomalous coupling describes that the standard model top-Higgs Yukawa coupling is deviated by a scale factor 'a' along with an extra pseudo-scalar type coupling parameterized by 'b'. For definiteness, we do not consider possible anomalous couplings of the Higgs with other fermions/bosons.

$\sqrt{S}$ (TeV)	$\sigma_{(1,0,1)}$ (fb)	$\sigma_{(1.2,0,1)}$ (fb)	$\sigma_{(0,\pm0.6,1)}$ (fb)	$\sigma_{(-0.4,\pm0.4,1)}$ (fb)	$\sigma_{(0.8,\pm0.3,1)}$ (fb)	$\sigma_{(1,0,0)}$ (fb)	$\sigma_{(1,0,2)}$ (fb)
8	6.18	14.70	2.67	7.19	4.84	13.18	2.87
14	26.50	62.51	10.26	27.83	21.57	54.22	12.76
33	167.51	391.56	57.91	157.88	122.02	328.67	83.85

Table 3. Higgs pair production cross sections for benchmark values of (a, b, κ) consistent with the LHC data. The parameter κ is the scale factor for the trilinear Higgs coupling defined below in the text. Numbers in 1st column stand for the standard model value, while the 5th column correspond to the best-fit value of the parameters.
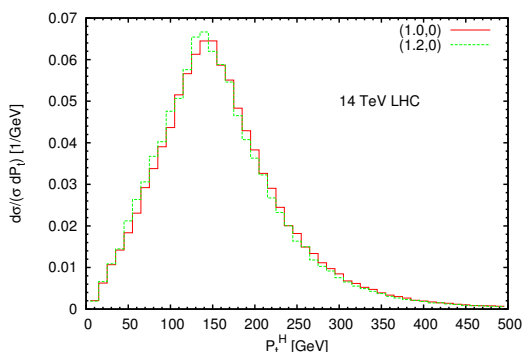
Figure 14. Comparison of normalized P_t-distributions of the Higgs for $a = 1.2, b = 0$ case and the standard model case.
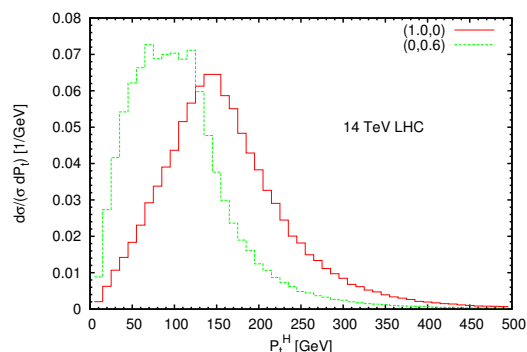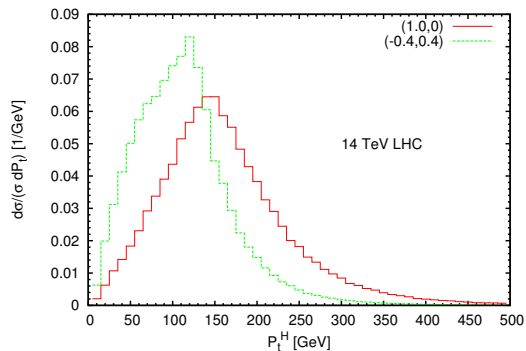

Figure 15. Comparison of normalized P_t-distributions of the Higgs for $a = 0, b = 0.6$ case and the standard model case.

In section 4, we have considered $O(1)$ deviations in the anomalous coupling parameters a and b from their standard model values. With such deviations one finds large enhancement in the Higgs pair production cross section. But this deviation can also contrast already gained knowledge on Higgs couplings on the basis of analyzed data at the LHC. Therefore, we constrain the parameter space by doing a global analysis based on data released by the ATLAS and CMS and show the allowed region in figure 13. The best-fit values obtained for the anomalous parameters are $(0.8, \pm0.3)$. Both the Higgs production via gluon fusion and its decay to digluon are affected more by b than by a. On the other hand, in the Higgs decay to diphoton, the deviation in a also plays an important role. We find that non-zero values of the pseudoscalar coupling parameter b are consistent with the data, but $a = -1$ case is completely ruled out at 95% CL. For $a = 1$, the parameter b is allowed to take any value between -0.4 to $+0.4$. Tight constrains on anomalous parameters indicate the consistency of LHC data with the standard model predictions. We would like to reiterate that the results of global analysis is not a sophisticated one. Once we introduce anomalous couplings of Higgs with other fermions/bosons, the allowed region of parameter space is likely to change.

Now and here, we again have a discussion on the double Higgs production after choosing four benchmark values of the parameters (a, b) which are allowed by the present LHC data.
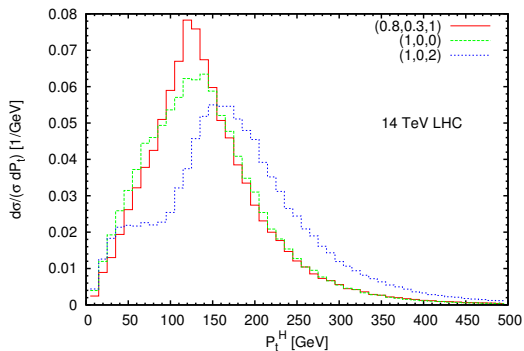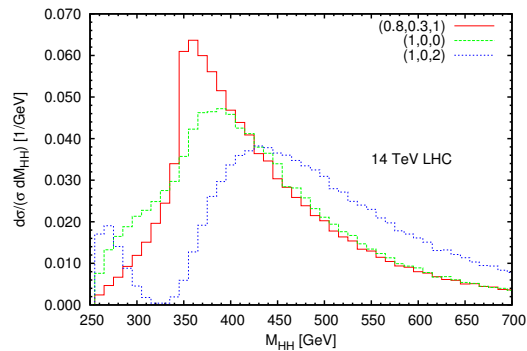
Figure 16. Comparison of normalized P_t-distributions of the Higgs for $a = -0.4, b = 0.4$ case and the standard model case.
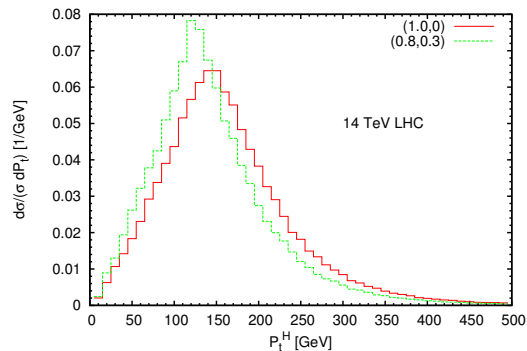
Figure 17. Comparison of normalized P_t-distributions of the Higgs for the best-fit values $a = 0.8, b = 0.3$ case and the standard model case.

Figure 18. Normalized P_t-distributions of the Higgs for various combinations of parameters (a, b, κ).


Figure 19. Normalized two Higgs invariant mass distributions for various combinations of (a, b, κ).

For these benchmark values, the two Higgs production cross sections at 8, 14 and 33 TeV center-of-mass energies are given in table 3. The table suggests that the cross section might get enhanced or reduced within the allowed parameter space. The Higgs P_t distributions in all the four cases are compared with the standard model case in figures 14–17. We have plotted them separately to emphasize the deviations in each case. These are consistent with the observations made in section 2. Like the deviations in P_t distributions, the deviations in invariant mass distributions M_{HH} are also not very large for $(1.2, 0)$ and $(0.8, 0.3)$ cases.

The double Higgs production process has also been studied in the context of anomalous trilinear Higgs coupling (λ_{HHH}). It is therefore important to investigate if there may be any overlap between the predictions due to the ttH anomalous coupling and those due to the anomalous trilinear Higgs coupling. We define the anomalous trilinear Higgs coupling using, $\lambda_{HHH} = \kappa \lambda_{HHH}^{\rm SM}$, where $\lambda_{HHH}^{\rm SM}$ is the standard model value of the coupling. Here we take, $\kappa = 0, 1, 2$ as possible values of the scale factor, $\kappa = 1$ being the standard model case. The Higgs pair production rates in presence of the anomalous trilinear Higgs coupling, are added in the last two columns of table 3. Note that in the case of $\kappa = 0$
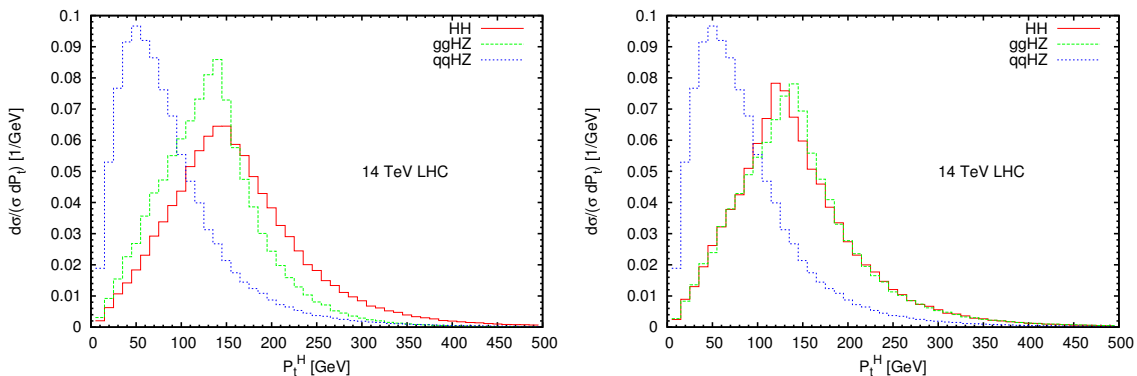
Figure 20. Comaprison of normalized P_t distributions of the Higgs pair production and HZ background processes. The contribution from quark-quark channel to $pp \to HZ$ is calculated at the tree level. The plot on the left is the standard model case, while the right one corresponds to the best-fit values $a = 0.8, b = 0.3$.

only the box amplitude contributes to the cross section. In $\kappa = 2$ case, the triangle contribution increases and the destructive interference between box and triangle amplitudes becomes more severe. The enhanced destructive interference effect, in this case, is visible in the kinematic distributions, shown in figures 18 and 19. In these figures, the kinematic distributions for $\kappa = 0$ and $\kappa = 2$ cases are compared with those for the best-fit values of (a, b). Due to characteristic differences in the distributions and very different values of cross sections, it should be possible to discriminate the case of the anomalous trilinear Higgs coupling from the case of the anomalous top-Higgs coupling. The possibility of the introduction of both the anomalous couplings may lead to more interesting situations.[6]

Out of many decay channels, the $HH \to b\bar{b}\gamma\gamma$ is the most promising channel to observe double Higgs production at the LHC. As described in the ref. [41], ZH production process is one of the main backgrounds in this channel. In the standard model, the tree-level cross section for $pp \to ZH$ at 14 TeV is about 0.63 pb and the K-factor at the next-to-next-to-leading order (NNLO) in QCD is close to 1.33 [88]. A part of the NNLO QCD contribution which arise due to the gluon-gluon fusion is also important at the LHC. Its cross section is ~ 100 fb at 14 TeV. In figure 20, we can see the relative importance of the gluon-gluon channel over the quark-quark channel in higher P_t region. Note that these distributions are normalized. Due to the much larger quark-quark channel contribution, the peak of the combined distribution does not shift from its tree-level position. A large P_t cut can be applied to suppress the contribution coming from the quark-quark channel. We also notice a significant overlap of the Higgs P_t distributions in $gg \to HH$ and $gg \to ZH$ cases in the standard model. The Higgs P_t distributions are also compared for the best-fit values of the parameters a and b in figure 20.

Diagrams contributing to $gg \to ZH$ amplitude are quite similar to the case of double Higgs production, however, only box diagram involves the top-Yukawa coupling. The gluon-

---

[6]In pure pseudoscalar ttH coupling case, the unpolarized cross section does not depend on the scale factor κ.

$\sqrt{S}$ (TeV)	$\sigma_{(1,0)}$ (fb)	$\sigma_{(1.2,0)}$ (fb)	$\sigma_{(0,\pm0.6)}$ (fb)	$\sigma_{(-0.4,\pm0.4)}$ (fb)	$\sigma_{(0.8,\pm0.3)}$ (fb)
8	24.72	20.35	63.58	80.96	31.01
14	97.98	79.42	275.36	355.74	126.08
33	569.60	454.15	1788.12	2346.59	756.69

Table 4. $gg \to ZH$ hadronic cross sections for allowed benchmark values of parameters (a, b). The kinematic settings in this case are same as in the two Higgs production case.

gluon channel to ZH production thus becomes very important background for the Higgs pair production process in presence of anomalous ttH coupling. The effect of anomalous top-Higgs coupling on the $gg \to ZH$ cross section at various collider center-of-mass energies are listed in table 4. The contributions from both the top and bottom quarks are included to cancel the anomaly in triangle diagram. Like the two Higgs production case, the box and triangle amplitudes interfere destructively in ZH case. The triangle amplitude, however, dominates the cross section. Due to this the cross section for the $(1.2, 0)$ case is smaller than the standard model cross section. We also note that non-zero b can introduce large enhancement in the cross section. In fact, the $gg \to HZ$ channel can be separately studied to probe the anomalous top-Higgs coupling at the LHC.

We have already seen that due to top-Higgs anomalous coupling, the P_t^H and M_{HH} distributions in the two Higgs production case shift towards low transverse momentum and low invariant mass regions. Referring back to the signal-background analysis performed in ref. [41] in $b\bar{b}\gamma\gamma$ channel, we note that the suggested cuts on P_t^H and M_{HH} may, therefore, not be effective in presence of anomalous ttH coupling. Nevertheless, cuts on η_H and η_{HH} may still be useful. Probing the effects of anomalous ttH coupling in the two Higgs production process at the LHC turns out to be a challenging task. It is clear that if we observe higher rates for the Higgs pair production at the LHC, it may not be only due to the top-Higgs anomalous coupling under consideration. It should be noted that large enhancement in the cross section can be realised only in some limited parameter space. Therefore, if lower production rates are observed this coupling can provide an explanation. This will require a more complete and detailed collider study which is beyond the scope of the present work.

Acknowledgments

References

[1] ATLAS collaboration, *Observation of a new particle in the search for the standard model Higgs boson with the ATLAS detector at the LHC*, *Phys. Lett.* **B 716** (2012) 1 [arXiv:1207.7214] [INSPIRE].

[2] CMS collaboration, *Observation of a new boson at a mass of* 125 *GeV with the CMS experiment at the LHC*, *Phys. Lett.* **B 716** (2012) 30 [arXiv:1207.7235] [INSPIRE].

[3] C. Grojean, E.E. Jenkins, A.V. Manohar and M. Trott, *Renormalization group scaling of Higgs operators and* $\Gamma(h->\gamma\gamma)$, *JHEP* **04** (2013) 016 [arXiv:1301.2588] [INSPIRE].

[4] K. Cheung, J.S. Lee and P.-Y. Tseng, *Higgs precision (higgcision) era begins*, *JHEP* **05** (2013) 134 [arXiv:1302.3794] [INSPIRE].

[5] J. Elias-Miró, J. Espinosa, E. Masso and A. Pomarol, *Renormalization of dimension-six operators relevant for the Higgs decays* $h \to \gamma\gamma, \gamma Z$, *JHEP* **08** (2013) 033 [arXiv:1302.5661] [INSPIRE].

[6] J. Ellis, V. Sanz and T. You, *Associated production evidence against Higgs impostors and anomalous couplings*, *Eur. Phys. J.* **C 73** (2013) 2507 [arXiv:1303.0208] [INSPIRE].

[7] P.P. Giardino, K. Kannike, I. Masina, M. Raidal and A. Strumia, *The universal Higgs fit*, arXiv:1303.3570 [INSPIRE].

[8] R. Contino, M. Ghezzi, C. Grojean, M. Muhlleitner and M. Spira, *Effective lagrangian for a light Higgs-like scalar*, *JHEP* **07** (2013) 035 [arXiv:1303.3876] [INSPIRE].

[9] J. Ellis and T. You, *Updated global analysis of Higgs couplings*, *JHEP* **06** (2013) 103 [arXiv:1303.3879] [INSPIRE].

[10] A. Djouadi and G. Moreau, *The couplings of the Higgs boson and its CP properties from fits of the signal strengths and their ratios at the* $7 + 8$ *TeV LHC*, arXiv:1303.6591 [INSPIRE].

[11] W.-F. Chang, W.-P. Pan and F. Xu, *Effective gauge-Higgs operators analysis of new physics associated with the Higgs boson*, *Phys. Rev.* **D 88** (2013) 033004 [arXiv:1303.7035] [INSPIRE].

[12] T. Corbett, O. éboli, J. Gonzalez-Fraile and M. Gonzalez-Garcia, *Determining triple gauge boson couplings from Higgs data*, *Phys. Rev. Lett.* **111** (2013) 011801 [arXiv:1304.1151] [INSPIRE].

[13] G. Isidori, A.V. Manohar and M. Trott, *Probing the nature of the Higgs-like Boson via* $h \to V\mathcal{F}$ *decays*, *Phys. Lett.* **B 728** (2014) 131 [arXiv:1305.0663] [INSPIRE].

[14] J. Elias-Miro, J. Espinosa, E. Masso and A. Pomarol, *Higgs windows to new physics through* $D = 6$ *operators: constraints and one-loop anomalous dimensions*, *JHEP* **11** (2013) 066 [arXiv:1308.1879] [INSPIRE].

[15] E.E. Jenkins, A.V. Manohar and M. Trott, *Renormalization group evolution of the standard model dimension six operators I: formalism and* λ *dependence*, *JHEP* **10** (2013) 087 [arXiv:1308.2627] [INSPIRE].

[16] M.B. Einhorn and J. Wudka, *Higgs-boson couplings beyond the standard model*, *Nucl. Phys.* **B 877** (2013) 792 [arXiv:1308.2255] [INSPIRE].

[17] A. Pomarol and F. Riva, *Towards the ultimate SM fit to close in on Higgs physics*, *JHEP* **01** (2014) 151 [arXiv:1308.2803] [INSPIRE].

[18] S. Banerjee, S. Mukhopadhyay and B. Mukhopadhyaya, *Higher dimensional operators and LHC Higgs data: the role of modified kinematics*, *Phys. Rev.* **D 89** (2014) 053010 [arXiv:1308.4860] [INSPIRE].

[19] E. Boos, V. Bunichev, M. Dubinin and Y. Kurihara, *Higgs boson signal at complete tree level in the SM extension by dimension-six operators*, *Phys. Rev.* **D 89** (2014) 035001 [arXiv:1309.5410] [INSPIRE].

[20] M. Klute, R. Lafaye, T. Plehn, M. Rauch and D. Zerwas, *Measuring Higgs couplings at a linear collider*, *Europhys. Lett.* **101** (2013) 51001 [arXiv:1301.1322] [INSPIRE].

[21] M. Klute, R. Lafaye, T. Plehn, M. Rauch and D. Zerwas, *Measuring Higgs couplings from LHC data*, *Phys. Rev. Lett.* **109** (2012) 101801 [arXiv:1205.2699] [INSPIRE].

[22] J. Adelman et al., *Top couplings: pre-Snowmass energy frontier 2013 overview*, arXiv:1309.1947 [INSPIRE].

[23] T.-F. Feng, X.-Q. Li and J. Maalampi, *The anomalous Higgs top couplings in the MSSM*, *Phys. Rev.* **D 69** (2004) 115007 [hep-ph/0310247] [INSPIRE].

[24] R. Frederix and F. Maltoni, *Top pair invariant mass distribution: a window on new physics*, *JHEP* **01** (2009) 047 [arXiv:0712.2355] [INSPIRE].

[25] E. Gabrielli and B. Mele, *Testing effective Yukawa couplings in Higgs searches at the Tevatron and LHC*, *Phys. Rev.* **D 82** (2010) 113014 [*Erratum ibid.* **D 83** (2011) 079901] [arXiv:1005.2498] [INSPIRE].

[26] S. Dawson, E. Furlan and I. Lewis, *Unravelling an extended quark sector through multiple Higgs production?*, *Phys. Rev.* **D 87** (2013) 014007 [arXiv:1210.6663] [INSPIRE].

[27] A. Pierce, J. Thaler and L.-T. Wang, *Disentangling dimension six operators through di-Higgs boson production*, *JHEP* **05** (2007) 070 [hep-ph/0609049] [INSPIRE].

[28] J.A. Aguilar-Saavedra, *A minimal set of top-Higgs anomalous couplings*, *Nucl. Phys.* **B 821** (2009) 215 [arXiv:0904.2387] [INSPIRE].

[29] C. Degrande, J. Gerard, C. Grojean, F. Maltoni and G. Servant, *Probing top-Higgs non-standard interactions at the LHC*, *JHEP* **07** (2012) 036 [*Erratum ibid.* **1303** (2013) 032] [arXiv:1205.1065] [INSPIRE].

[30] E.W.N. Glover and J.J. van der Bij, *Higgs boson pair production via gluon fusion*, *Nucl. Phys.* **B 309** (1988) 282 [INSPIRE].

[31] O.J.P. Eboli, G.C. Marques, S.F. Novaes and A.A. Natale, *Twin Higgs boson production*, *Phys. Lett.* **B 197** (1987) 269 [INSPIRE].

[32] D. Binosi, J. Collins, C. Kaufhold and L. Theussl, *JaxoDraw: a graphical user interface for drawing feynman diagrams. Version 2.0 release notes*, *Comput. Phys. Commun.* **180** (2009) 1709 [arXiv:0811.4113] [INSPIRE].

[33] S. Kanemura and K. Tsumura, *Effects of the anomalous Higgs couplings on the Higgs boson production at the large hadron Collider*, *Eur. Phys. J.* **C 63** (2009) 11 [arXiv:0810.0433] [INSPIRE].

[34] R. Contino et al., *Anomalous couplings in double Higgs production*, *JHEP* **08** (2012) 154 [arXiv:1205.5444] [InSPIRE].

[35] F. Goertz, A. Papaefstathiou, L.L. Yang and J. Zurita, *Higgs boson self-coupling measurements using ratios of cross sections*, *JHEP* **06** (2013) 016 [arXiv:1301.3492] [InSPIRE].

[36] A.J. Barr, M.J. Dolan, C. Englert and M. Spannowsky, *Di-Higgs final states augMT2ed — Selecting hh events at the high luminosity LHC*, *Phys. Lett.* **B 728** (2014) 308 [arXiv:1309.6318] [InSPIRE].

[37] T. Plehn, M. Spira and P. Zerwas, *Pair production of neutral Higgs particles in gluon-gluon collisions*, *Nucl. Phys.* **B 479** (1996) 46 [*Erratum ibid.* **B 531** (1998) 655] [hep-ph/9603205] [InSPIRE].

[38] C.O. Dib, R. Rosenfeld and A. Zerwekh, *Double Higgs production and quadratic divergence cancellation in little Higgs models with T parity*, *JHEP* **05** (2006) 074 [hep-ph/0509179] [InSPIRE].

[39] J.-J. Liu, W.-G. Ma, G. Li, R.-Y. Zhang and H.-S. Hou, *Higgs boson pair production in the little Higgs model at hadron collider*, *Phys. Rev.* **D 70** (2004) 015001 [hep-ph/0404171] [InSPIRE].

[40] S. Dawson, S. Dittmaier and M. Spira, *Neutral Higgs boson pair production at hadron colliders: QCD corrections*, *Phys. Rev.* **D 58** (1998) 115012 [hep-ph/9805244] [InSPIRE].

[41] J. Baglio et al., *The measurement of the Higgs self-coupling at the LHC: theoretical status*, *JHEP* **04** (2013) 151 [arXiv:1212.5581] [InSPIRE].

[42] D.Y. Shao, C.S. Li, H.T. Li and J. Wang, *Threshold resummation effects in Higgs boson pair production at the LHC*, *JHEP* **07** (2013) 169 [arXiv:1301.1245] [InSPIRE].

[43] J. Grigo, J. Hoff, K. Melnikov and M. Steinhauser, *On the Higgs boson pair production at the LHC*, *Nucl. Phys.* **B 875** (2013) 1 [arXiv:1305.7340] [InSPIRE].

[44] D. de Florian and J. Mazzitelli, *Higgs boson pair production at next-to-next-to-leading order in QCD*, *Phys. Rev. Lett.* **111** (2013) 201801 [arXiv:1309.6594] [InSPIRE].

[45] E. Asakawa, D. Harada, S. Kanemura, Y. Okada and K. Tsumura, *Higgs boson pair production in new physics models at hadron, lepton and photon colliders*, *Phys. Rev.* **D 82** (2010) 115002 [arXiv:1009.4670] [InSPIRE].

[46] A. Djouadi, W. Kilian, M. Muhlleitner and P. Zerwas, *The reconstruction of trilinear Higgs couplings*, hep-ph/0001169 [InSPIRE].

[47] V. Barger, M. McCaskey and G. Shaughnessy, *Single top and Higgs associated production at the LHC*, *Phys. Rev.* **D 81** (2010) 034020 [arXiv:0911.1556] [InSPIRE].

[48] S. Biswas, E. Gabrielli and B. Mele, *Single top and Higgs associated production as a probe of the Htt coupling sign at the LHC*, *JHEP* **01** (2013) 088 [arXiv:1211.0499] [InSPIRE].

[49] M. Farina, C. Grojean, F. Maltoni, E. Salvioni and A. Thamm, *Lifting degeneracies in Higgs couplings using single top production in association with a Higgs boson*, *JHEP* **05** (2013) 022 [arXiv:1211.3736] [InSPIRE].

[50] P. Agrawal, S. Mitra and A. Shivaji, *Effect of anomalous couplings on the associated production of a single top quark and a Higgs boson at the LHC*, *JHEP* **12** (2013) 077 [arXiv:1211.4362] [InSPIRE].

[51] V. Koulovassilopoulos and R.S. Chivukula, *The phenomenology of a nonstandard Higgs boson in $W(L)W(L)$ scattering*, *Phys. Rev.* **D 50** (1994) 3218 [hep-ph/9312317] [INSPIRE].

[52] E. Accomando et al., *Workshop on CP studies and non-standard Higgs physics*, hep-ph/0608079 [INSPIRE].

[53] W. Bernreuther, A. Brandenburg and M. Flesch, *Effects of Higgs sector CP-violation in top quark pair production at the LHC*, hep-ph/9812387 [INSPIRE].

[54] K. Whisnant, B.-L. Young and X. Zhang, *Unitarity and anomalous top quark Yukawa couplings*, *Phys. Rev.* **D 52** (1995) 3115 [hep-ph/9410369] [INSPIRE].

[55] X. Zhang, S. Lee, K. Whisnant and B. Young, *Phenomenology of a nonstandard top quark Yukawa coupling*, *Phys. Rev.* **D 50** (1994) 7042 [hep-ph/9407259] [INSPIRE].

[56] J. Shu and Y. Zhang, *Impact of a CP-violating Higgs: from LHC to Baryogenesis*, *Phys. Rev. Lett.* **111** (2013) 091801 [arXiv:1304.0773] [INSPIRE].

[57] J. Brod, U. Haisch and J. Zupan, *Constraints on CP-violating Higgs couplings to the third generation*, *JHEP* **11** (2013) 180 [arXiv:1310.1385] [INSPIRE].

[58] R. Godbole, C. Hangst, M. Muhlleitner, S. Rindani and P. Sharma, *Model-independent analysis of Higgs spin and CP properties in the process $e^+e^- \to t\bar{t}\Phi$*, *Eur. Phys. J.* **C 71** (2011) 1681 [arXiv:1103.5404] [INSPIRE].

[59] C.R. Schmidt and M.E. Peskin, *A probe of CP-violation in top quark pair production at hadron supercolliders*, *Phys. Rev. Lett.* **69** (1992) 410 [INSPIRE].

[60] J. Ellis, D.S. Hwang, K. Sakurai and M. Takeuchi, *Disentangling Higgs-top couplings in associated production*, arXiv:1312.5736 [INSPIRE].

[61] J.A.M. Vermaseren, *New features of FORM*, math-ph/0010025 [INSPIRE].

[62] G.J. van Oldenborgh and J.A.M. Vermaseren, *New algorithms for one loop integrals*, *Z. Phys.* **C 46** (1990) 425 [INSPIRE].

[63] A. van Hameren, *OneLOop: for the evaluation of one-loop scalar functions*, *Comput. Phys. Commun.* **182** (2011) 2427 [arXiv:1007.4716] [INSPIRE].

[64] P.M. Nadolsky et al., *Implications of CTEQ global analysis for collider observables*, *Phys. Rev.* **D 78** (2008) 013004 [arXiv:0802.0007] [INSPIRE].

[65] ATLAS collaboration, *Search for the Standard Model Higgs boson in the $H \to Z\gamma$ decay mode with pp collisions at $\sqrt{s} = 7$ and 8 TeV*, ATLAS-CONF-2013-009 (2013).

[66] CMS collaboration, *Search for a Higgs boson decaying into a Z and a photon in pp collisions at $\sqrt{s} = 7$ and 8 TeV*, CMS-HIG-13-006 (2013).

[67] A. Djouadi, *The anatomy of electro-weak symmetry breaking. II. The Higgs bosons in the minimal supersymmetric model*, *Phys. Rept.* **459** (2008) 1 [hep-ph/0503173] [INSPIRE].

[68] P.P. Giardino, K. Kannike, M. Raidal and A. Strumia, *Reconstructing Higgs boson properties from the LHC and Tevatron data*, *JHEP* **06** (2012) 117 [arXiv:1203.4254] [INSPIRE].

[69] N.D. Christensen and C. Duhr, *FeynRules — Feynman rules made easy*, *Comput. Phys. Commun.* **180** (2009) 1614 [arXiv:0806.4194] [INSPIRE].

[70] C. Degrande et al., *UFO — The Universal FeynRules Output*, *Comput. Phys. Commun.* **183** (2012) 1201 [arXiv:1108.2040] [INSPIRE].

[71] J. Alwall, M. Herquet, F. Maltoni, O. Mattelaer and T. Stelzer, *MadGraph 5: going beyond*, *JHEP* **06** (2011) 128 [arXiv:1106.0522] [INSPIRE].

[72] ATLAS collaboration, *Measurements of the properties of the Higgs-like boson in the two photon decay channel with the ATLAS detector using* $25\,fb^{-1}$ *of proton-proton collision data*, ATLAS-CONF-2013-012 (2013).

[73] ATLAS collaboration, *Measurements of the properties of the Higgs-like boson in the four lepton decay channel with the ATLAS detector using* $25\,fb^{-1}$ *of proton-proton collision data*, ATLAS-CONF-2013-013 (2013).

[74] ATLAS collaboration, *Measurements of the properties of the Higgs-like boson in the* $WW^{(*)} \to \ell\nu\ell\nu$ *decay channel with the ATLAS detector using* $25\,fb^{-1}$ *of proton-proton collision data*, ATLAS-CONF-2013-030 (2013).

[75] CMS collaboration, *Updated measurements of the Higgs boson at* $125\,GeV$ *in the two photon decay channel*, CMS-PAS-HIG-13-001 (2013).

[76] CMS collaboration, *Properties of the Higgs-like boson in the decay* $H \to ZZ \to 4l$ *in pp collisions at* $\sqrt{s} = 7$ *and* $8\,TeV$, CMS-PAS-HIG-13-002 (2013).

[77] CMS collaboration, *Evidence for a particle decaying to* W^+W^- *in the fully leptonic final state in a standard model Higgs boson search in pp collisions at the LHC*, CMS-PAS-HIG-13-003 (2013).

[78] CMS collaboration, *Higgs to bb in the VBF channel*, CMS-PAS-HIG-13-011 (2013).

[79] ATLAS collaboration, *Search for the bb decay of the standard model Higgs boson in associated W/ZH production with the ATLAS detector*, ATLAS-CONF-2013-079 (2013).

[80] CMS collaboration, *Search for the standard model Higgs boson produced in association with W or Z bosons, and decaying to bottom quarks for LHCp 2013*, CMS-PAS-HIG-13-012 (2013).

[81] ATLAS collaboration, *Search for ttH production in the* $H \to yy$ *channel at* $\sqrt{s} = 8\,TeV$ *with the ATLAS detector*, ATLAS-CONF-2013-080 (2013).

[82] ATLAS collaboration, *Search for the standard model Higgs boson produced in association with top quarks in proton-proton collisions at* $\sqrt{s} = 7$ *TeV using the ATLAS detector*, ATLAS-CONF-2012-135 (2012).

[83] CMS collaboration, *Search for ttH production in events where H decays to photons at* $8\,TeV$ *collisions*, CMS-PAS-HIG-13-015 (2013).

[84] CMS collaboration, *Search for the standard model Higgs boson produced in association with a top-quark pair in pp collisions at the LHC*, CMS-HIG-12-035 (2013).

[85] T. Kakuda, K. Nishiwaki, K.-y. Oda and R. Watanabe, *Universal extra dimensions after Higgs discovery*, *Phys. Rev.* **D 88** (2013) 035007 [arXiv:1305.1686] [INSPIRE].

[86] T. Abe et al., *Minimal dilaton model*, *Phys. Rev.* **D 86** (2012) 115016 [arXiv:1209.4544] [INSPIRE].

[87] G. Gómez-Ceballos, *Study of standard model scalar production in bosonic decay channels in CMS*, talk given at *Rencontres de Moriond ElectroWeak*, March 2–9, La Thuile, Italy (2013).

[88] LHC HIGGS CROSS SECTION WORKING GROUP, S. Dittmaier et al., *Handbook of LHC Higgs cross sections: 1. Inclusive observables*, arXiv:1101.0593 [INSPIRE].